Magnetic study of the Furnas caldera (Azores)

Isabel Blanco, Alicia García and J. Miquel Torta
Departamento de Volcanología, Museo Nacional de Ciencias Naturales, CSIC, Madrid, Spain

Abstract
A local ground magnetic study of the Furnas caldera (S. Miguel Island, Azores) has provided new insight into the magnetic structure of this volcano. Analysis of the data comprised removal of the IGRF, reduction to the pole, pseudogravity integration and upward continuation. Also, a spectral method was applied to estimate the depth to the magnetic sources, as well as a 2.5D forward modelling technique. Magnetic properties obtained at the laboratory for some representative sample rocks were considered in the modelling process. The most relevant features are the existence of an important negative anomaly inside the caldera and of an intense positive anomaly to the south of the coast. The former points out a decrease in the magnetization of the caldera filling materials with respect to the surrounding rocks, which could be explained as the result of post-eruption processes such as hydrothermal alteration. This is expected as Furnas has an active hydrothermal system probably related with a magmatic reservoir at high temperature. The positive anomaly suggests the existence of a strongly-magnetized body beneath the south coast.

Key words *Furnas caldera – magnetic anomalies – hydrothermal alteration*

1. Introduction

Furnas is one of the three active quaternary stratovolcanoes on the island of S. Miguel, in the Azores Archipelago. It consists of a multicyclic caldera which last erupted in 1630 A.D. The activity of this volcano has been mainly explosive. At present, there are important fumarolic emissions linked to the presence of an active hydrothermal system. Furnas was selected by the European Union as one of the six laboratory volcanoes included in the «Climatology and Natural Hazards» programme in 1991. A multidisciplinary research was planned aimed at obtaining information on the activity of this volcano, its eruptive history and its structure. This latter topic was considered in the geophysics subproject, which included a magnetic survey.

The study of the magnetic anomalies is considered a useful method for the structural investigation of recent volcanic areas, since volcanic rocks are generally characterized by high magnetizations. Magnetization contrasts in these zones have different origins: high temperature rocks, volcano-tectonic structures, shallow or deep magmatic chambers, intrusions, difference in the amount of lavas and pyroclasts, reversed or normal magnetized rocks, hydrothermal alterations, etc. (Lenat and Aubert, 1982). Thus, magnetic studies are a common technique in the geophysical investigation of volcanic areas (*e.g.*, Lenat and Aubert, 1982; Nishida and Miyajima, 1984; Hildebrand *et al.*, 1993; Barberi *et al.*, 1994;

Mailing address: Dr. Isabel Blanco, Departamento de Volcanología, Museo Nacional de Ciencias Naturales, Consejo Superior de Investigaciones Científicas, José Gutiérrez Abascal 2, 28006 Madrid, España; e-mail: mcnbm72@pinar1.csic.es

Okubo, 1994). However, few of them deal with structural studies of caldera complexes (Muroi, 1973; Nishida, 1984; Ortiz *et al.*, 1992; Okubo and Shibuya, 1993; Campos-Enriquez and Garduño-Monroy, 1995).

Furnas cannot be considered a well-studied volcano, especially from the geophysical point of view. As far as we know, the only paper dealing with its structure is that of Machado (1973), who made a simplistic interpretation of the gravimetric and aeromagnetic maps of S. Miguel Island compiled during the 60's (Coelho, 1968; Quintino, 1962). According to this author, S. Miguel Island is crossed by the Mid-Atlantic Ridge; consequently, positive and negative magnetic anomalies detected over the island correspond to the normal and reversed polarity zones associated with the crustal generation from this spreading center. In the 80's, interest in exploiting geothermal resources of S. Miguel promoted some geophysical research. However, these studies were almost exclusively focused on the neighbouring volcano Fogo-Agua de Pau. Only an audio-magnetotelluric survey was carried out on Furnas (Hoover *et al.*, 1983), detecting very shallow (tens of meters) resistivity anomalies linked to fumaroles. This paper describes a magnetic survey, the techniques used to produce the magnetic anomaly maps and the results obtained concerning the causative bodies. These results, integrated with those from other geophysical and geological techniques, contribute to a better understanding of this volcano.

2. Geologic setting

The Azores Archipelago is located in the Atlantic, where the American, Eurasian and African lithospheric plates meet (Krause and Watkins, 1970; Forjaz, 1984). Three main tectonic features characterize the geodynamics of this part of the North Atlantic: a) the Mid-Atlantic Ridge which crosses the Archipelago between the islands of Flores and Faial (Krause and Watkins, 1970); b) the East Azores Fracture Zone which extends E-W from the Mid-Atlantic Ridge to Gibraltar (Krause and Watkins, 1970); c) the Terceira Rift or Azores Fracture Zone which extends from the island of Santa María towards the Mid-Atlantic Ridge following approximately a NW trend (Machado, 1959). Also, there is an important fault system which crosses the islands of Faial-Pico and San Jorge, which have a general WNW-ESE trend and converge with the Terceira Rift at the western end of São Miguel (fig. 1).

São Miguel Island is located over the Azores Fracture Zone and is the biggest island, covering an area of approximately 65×15 km^2 (fig. 2). The oldest materials are found in the Nordeste volcanic complex, with an age of 4 Ma. At present, three active stratovolcanoes exist on this island: Sete Cidades, Agua de Pau or Fogo and Furnas. All three volcanoes have calderas that formed in the Late Pleistocene as a consequence of voluminous eruptions of trachytic pyroclastic flows and fall deposits.

Furnas volcano, located between the volcanoes of Fogo and Povoaçao (the last one considered extinct), was constructed almost entirely during the last 100000 years (Moore, 1991). The present caldera, with a size of 7×4.5 km (N-S, E-W directions, respectively) and flanked by steep walls as high as 500 m, was formed after several different collapse episodes, the last being about 5000 years ago (Guest *et al.*, 1994). These collapses were followed by caldera filling eruptions. It is known that Furnas erupted explosively at least ten times during the last 5000 years (Booth *et al.*, 1978). Two of these eruptions are historic, one in the mid fifteenth century and the other in 1630 A.D. The latter buried the south rim of the caldera and destroyed the village of Furnas. A detailed geologic mapping of Furnas volcano was performed by Moore (1983, 1991). Trachyte is the most abundant type of rock, as it constitutes more than 83% of the total volume of Furnas.

An active hydrothermal system exists as well as important fumarolic emissions. This indicates the presence of a magmatic body at high temperature within the caldera, the existence of which is postulated by several authors (Machado, 1973; Booth *et al.*, 1978; Forjaz, 1986; Moore, 1991). A system of active normal faults crosses the caldera following a WNW-ESE direction. A second important tec-

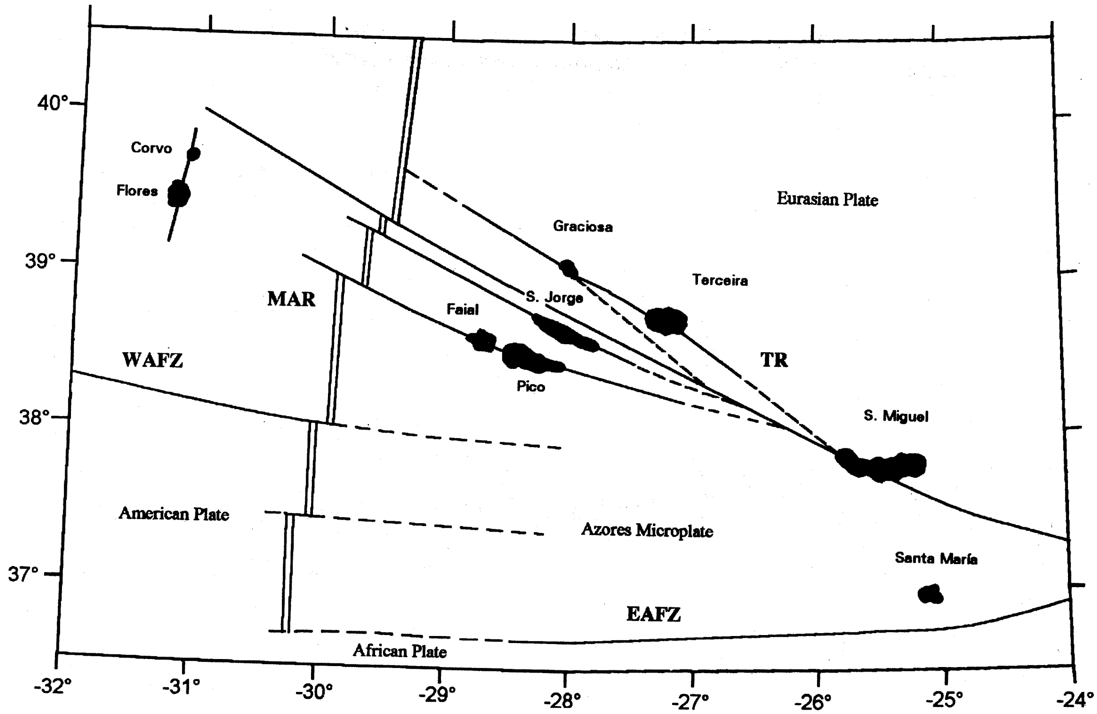

Fig. 1. Geodynamical framework of the Azores Archipelago. WAFZ = West Azores Fracture Zone; EAFZ = East Azores Fracture Zone; MAR = Mid-Atlantic Ridge; TR = Terceira Rift (after Forjaz, 1984).

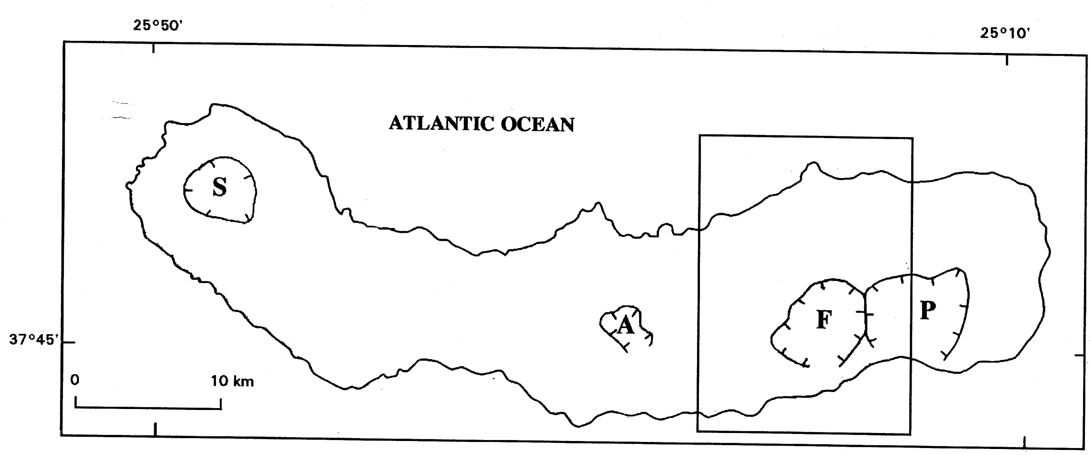

Fig. 2. Map of São Miguel Island. Hatched lines mark the calderas: S = Sete Cidades; A = Agua de Pau or Fogo; F = Furnas; P = Povoaçao. The square shows the area covered by the land magnetic survey.

tonic trend ranges from N-S to NE-SW and comprises a complete set of conjugate normal slip faults (Guest *et al.*, 1994; Gaspar *et al.*, 1996).

3. Data acquisition and reduction

Magnetic total intensity was measured in two field surveys (1993-1994). A total of 473 points were measured using a proton precession magnetometer (resolution 0.1 nT), covering the area marked in fig. 2 (about 15×15 km^2).

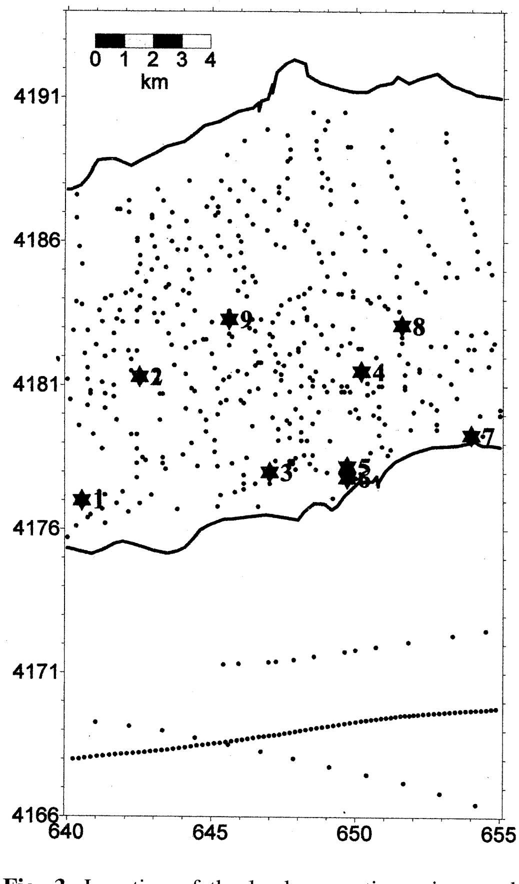

Fig. 3. Location of the land magnetic stations and the selected marine profiles (dots). The outcrops where the rock samples were collected are also shown (stars). Coordinates are UTM (km).

Latitude and longitude of each point were measured with a portable GPS receiver. A reference station was deployed at the Ermita Nosa Señora da Paz, to the North of Vila Franca village (outside the area of the study). Distance between stations was selected to be about 500 m, especially in the immediate neighbourhood of the caldera, although the distribution of the data points is not regular in some areas because of the rugged topography and the dense vegetation (fig. 3). Land data were completed with some US NGDC marine profiles located near the south coast of the island, in order to better define marine anomalies. Some rock samples were collected from the most representative outcrops of the volcano in order to study their magnetic properties (magnetic susceptibility, remanence, Curie temperature). These results were used as reference values when modelling the deep structures that generate the magnetic anomalies.

The data reduction process included removal of the external field variations and subtraction of the core field applying the IGRF model (IAGA, 1992). After this, the data were gridded at a constant spacing of 0.5 km using a minimum curvature algorithm. The resulting map is shown in fig. 4.

4. Rock magnetic properties

Crustal magnetic anomalies reflect the spatial variation of the total magnetization of rocks. To understand the origin of this variability it is necessary to know the magnetic properties of the rocks and the factors that control them. This is essential to the reliable geological explanation of the observed magnetic anomalies.

Total magnetization, M_T, is the sum of two vectors: remanent magnetization, M_{NRM} (NRM: Natural Remanent Magnetization), and induced magnetization, M_{IND}. That is, $M_T = M_{\mathrm{NRM}} + M_{\mathrm{IND}} = M_{\mathrm{NRM}} + \chi/\mu\, B$, where χ is the magnetic susceptibility of the rock, μ is the magnetic permeability and B is the Earth's magnetic induction. In volcanic rocks, NRM is called TRM, thermal remanent magnetization, as remanence is primarily acquired when

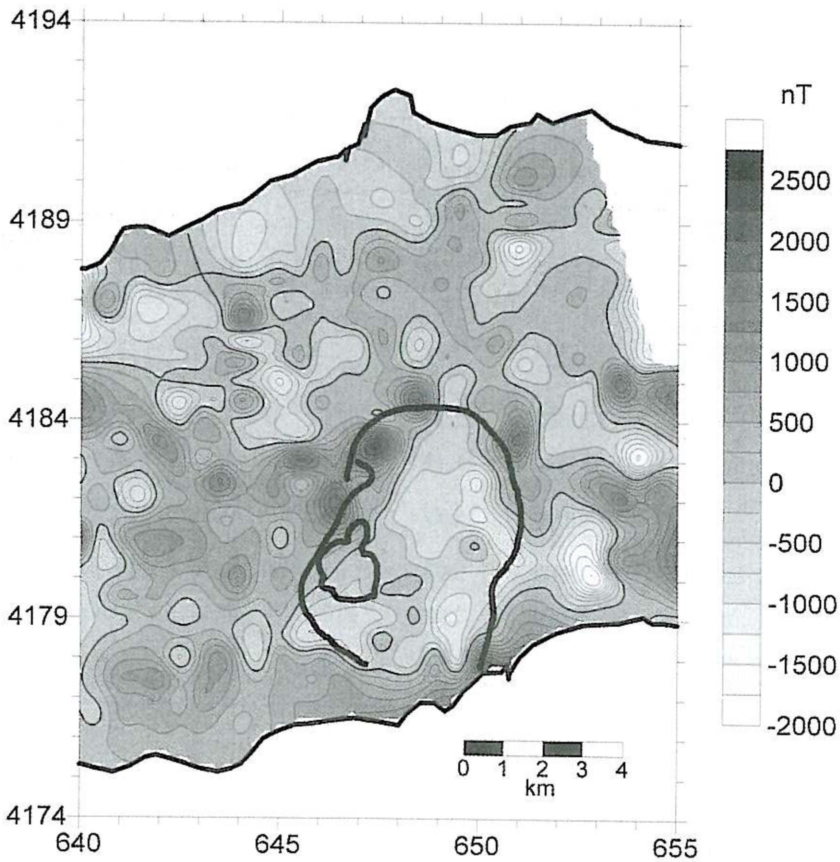

Fig. 4. Magnetic anomaly map of Furnas caldera and surrounding areas obtained from the land magnetic data. As in the next figures, the thick black line marks the caldera rim and the Lagoa das Furnas outline. Coordinates are UTM (km).

erupted rocks cool below their Curie temperature. Both χ and M_{NRM} essentially depend on the amount, grain size and composition of titanomagnetite, which is the main carrier of magnetization in volcanic rocks (Reynolds *et al.*, 1990). The variation of these properties is a consequence of magma composition, cooling rate, volatile content and alteration history (Hildebrand *et al.*, 1993). Volcanic rocks are usually characterized by a high remanence-to-induction ratio ($M_{NRM}/M_{IND} = Q$, Koenigsberger ratio). This is due to the small grains of magnetic minerals typical for these rocks (produced by high-temperature alteration processes), which generally implies high remanence and low susceptibility (Watkins and Paster, 1971).

Different processes can alter the magnetic properties of primary titanomagnetite: mineral ex-solution, high-temperature oxidation, low-temperature oxidation and hydrothermal alteration (*e.g.*, Haggerty, 1979; Reynolds, 1990). It is necessary to know what type and degree of alteration have affected the rocks in order to obtain an appropriate explanation of the variations in total magnetization detected by means of magnetic anomaly studies. For example, both ex-solution and high-temperature oxida-

Table I. Magnetic properties measured in the laboratory for the rock samples collected from the outcrops shown in fig. 4. M_{NRM} is Natural Remanent Magnetization; χ is initial magnetic susceptibility; M_{IND} is induced magnetization (assuming a magnetic field intensity of 34.7 Am^{-1}); Q is Koenigsberger ratio (M_{NRM}/M_{IND}); M_{TOT} is the sum of M_{NRM} plus M_{IND} (supposed to be parallel) and T_C is the Curie temperature.

Sample	Rock type	Age (years)	M_{NRM} (Am^{-1})	χ (10^{-6} SI)	M_{IND} (Am^{-1})	Q	M_{TOT} (Am^{-1})	T_C (°C)
1	Trachytic pumice	5000	0.09	9.5	0.05	1.8	0.14	225
2	Hawaiitic stromb. pyroclast	11500	1.25	7.3	0.04	31.2	1.29	515
3	Trachytic pumice (1630 A.D. historic eruption)	364	0.01	2.5	0.01	1.0	0.02	270
4	Trachyte	120000	2.27	175.2	0.96	2.4	3.23	260
5	Trachytic dyke	28000	1.41	108.4	0.59	2.4	2.00	450
6	Basalt	750000	15.39	165.6	0.91	16.9	16.30	400 580
7	Trachytic ignimbrite	640000	6.07	65.3	0.36	16.9	6.43	580
8	Hawaiite	75000	3.41	810.1	4.43	0.8	7.84	530
9	Hawaiitic stromb. pyroclast	17000	0.45	5.0	0.03	15.0	0.48	280

tion favour the decrease of the titanium content of titanomagnetite and therefore lead to increases in magnetization, Curie temperature and magnetic stability. Advanced high-temperature oxidation of magnetite + ilmenite, nevertheless, creates weakly magnetic hematite. Low-temperature oxidation of magnetite-ulvospinel to titanomaghemite causes a decrease in magnetization and an increase in Curie temperature, while low-temperature oxidation of low-titanium magnetite to hematite greatly diminishes magnetization (Reynolds *et al.*, 1990). The effect of hydrothermal alteration is not known likewise, but it generally leads to a decrease of magnetization and a rise in the Curie point.

The rock samples collected in the field were analyzed in the laboratory for the determination of their magnetic susceptibility, remanent magnetization and Curie temperature (table I). The location of the outcrops are marked in fig. 4. The samples include five trachytes (two pumices, one dyke, one ignimbrite and one lava), three hawaiites (two pyroclasts and one lava) and one basalt (lava). Both susceptibility and remanent magnetization appear to be very variable. The lowest values correspond, as expected, to the pumices (samples 1, 3) and the pyroclasts (samples 2, 9). The hawaiite (sample 8) shows the greatest susceptibility, five times greater than for the rest of the trachytes and the basalt. The high value of remanence of the trachytic ignimbrite (sample 7) and, especially, of the basalt (sample 6), must be highlighted. The Koenigsberger ratio is greater than 1 for most rocks, with only one exception (sample 8). The highest value corresponds to sample 2, with a ratio of more than 30. It is noteworthy that Q is low for the trachytes compared to the rest of rocks. This was also observed by Nunziata and Rapolla (1987) on the island of Ischia (Italy). Total magnetization was calculated assuming that both remanent and induced magnetization are parallel, taking into account the ages of the rocks. The basalt (sample 6) is the most strongly magnetized rock, followed by the hawaiite (sample 8) and the ignimbrite (sample 7). The Curie points were obtained from the curves of susceptibility *versus* temperature, heating the samples from 0°C to 700°C. They range from 225°C to 580°C. This suggests that the main carriers of the magnetization are titanomagnetites with different degrees of oxidation.

The values measured for the magnetic parameters, especially those of the trachytes, will be used for the interpretation of the anomalies which will be discussed later. However, the small number of samples and the evidence of an active hydrothermal system (which modifies the physical properties of the rocks within the caldera) must be considered, so that the results mentioned here may not be representative of all the materials in Furnas.

5. Interpretative techniques

In order to clarify the magnetic anomaly map and obtain some information on the

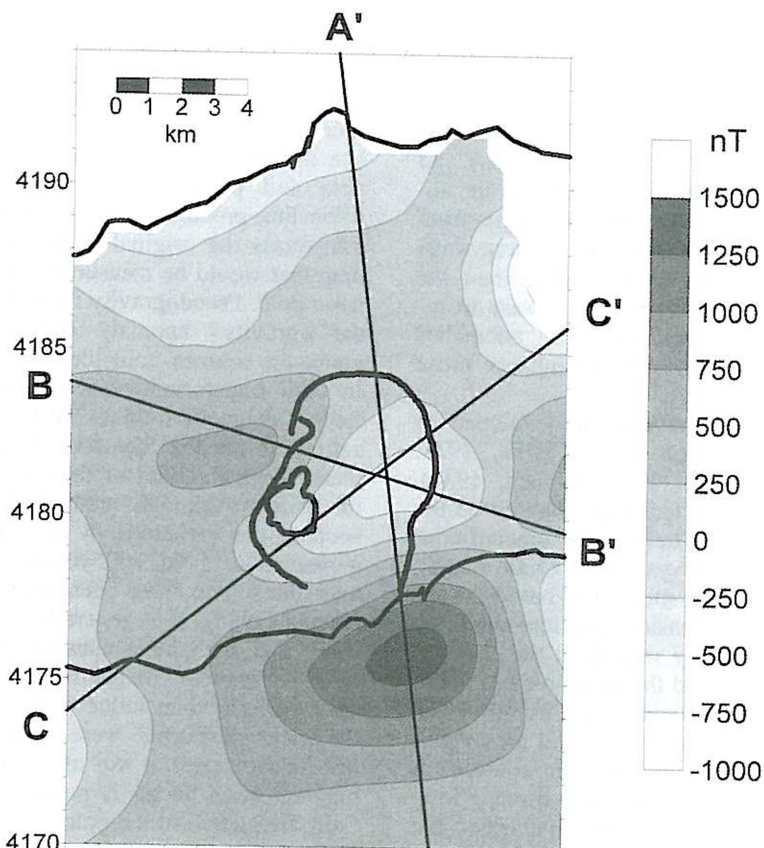

Fig. 5. Upward continuation to 2 km a.s.l. of the magnetic anomaly map of Furnas caldera and surrounding areas obtained from land and marine data. The black lines correspond to the profiles selected for the spectral analysis and for the forward modelling.

sources, different interpretative techniques were applied to the data. Upward continuation was performed for the filtering of terrain effects; reduction to the pole and pseudogravity integration were applied to shift anomalies above their sources; a simple spectral inversion method was used to define magnetic layers. Finally, bearing in mind all the information provided by this techniques, a structural model was constructed along a selecleed profile.

5.1. *Upward continuation and terrain effects*

One important problem derived from the high magnetizations that usually characterize young volcanic rocks is that many of the measured anomalies are often originated by the unevenness of the relief. Sometimes, these shallow anomalies are so high that they mask and distort deeper ones. In Furnas volcano the topography is rugged, as the altitude ranges from sea level to almost 1000 m. The caldera walls are, at some points, 500 m higher than the inner ground. Therefore, it is necessary to remove or, at least, attenuate the anomalies caused by the relief in order to enhance those due to deeper sources.

Several methods have been developed to perform this correction (*e.g.*, Clarke, 1971; Plouff, 1976; Blakely, 1981; Grauch, 1987). One of the traditional techniques, based on the application of linear filters, is the upward continuation (Bhattacharyya and Chan, 1977; Jacobsen, 1987). This method is based on the property that the extension and magnitude of the anomaly is closely related to the distance between the source and the measurement point. Therefore, shallow anomalies are usually characterized by short-wavelengths and are attenuated as we move away from the sources. A similar result would be obtained using a low-pass filter. This method is effective when the topographic anomalies and the target anomalies are characterized by quite different wavelengths. However, short-wavelength anomalies that could be important may be removed and, on the contrary, long-wavelength anomalies of topographic origin may be maintained.

Taking into account that recent volcanics are usually reflected on the magnetic anomaly maps as short-wavelength anomalies, upward continuation was applied to remove terrain effects. The program TRSMAP (Gibert and Galdeano, 1985) was used. After performing the continuation to several heights, an altitude of 2 km a.s.l. was selected. The upwardly-continued map appears in fig. 5.

5.2. *Reduction to the pole and pseudogravity*

The dipolar character of magnetic anomalies, especially at low and temperate latitudes, makes their interpretation more difficult than, for example, gravity anomalies. This means that magnetic anomalies are shifted with respect to the sources, so it is not evident to relate the former to the latter. Reduction to the pole and pseudogravity integration help to solve this problem (Baranov, 1957). The first transforms the original map into the anomaly map that would be measured in the north magnetic pole. Pseudogravity integration calculates the «gravity» anomaly map assuming that magnetic sources coincide with gravity ones. In both transformations the directions of the Earth's magnetic field and of the total magnetization are needed. The former can be approximated with a model of the core field such as the IGRF. Although methods for taking into account the variations in the direction of the geomagnetic field and of the magnetization over the region have been attempted (Arkani-Hamed, 1988), it is generally necessary to assume that both have constant directions. Because remanent magnetization is generally much greater than induced magnetization and the rocks of Furnas were emplaced after the last field reversal, it was assumed that the total magnetization vector is parallel to the present field. Reduction to the pole was applied to land survey data in order to enhance shallow anomalies (fig. 6a). Pseudogravity transformation was applied to both land and marine data after upward continuation was made (fig. 7). Thus, deeper anomalies will be interpreted and modelled more easily.

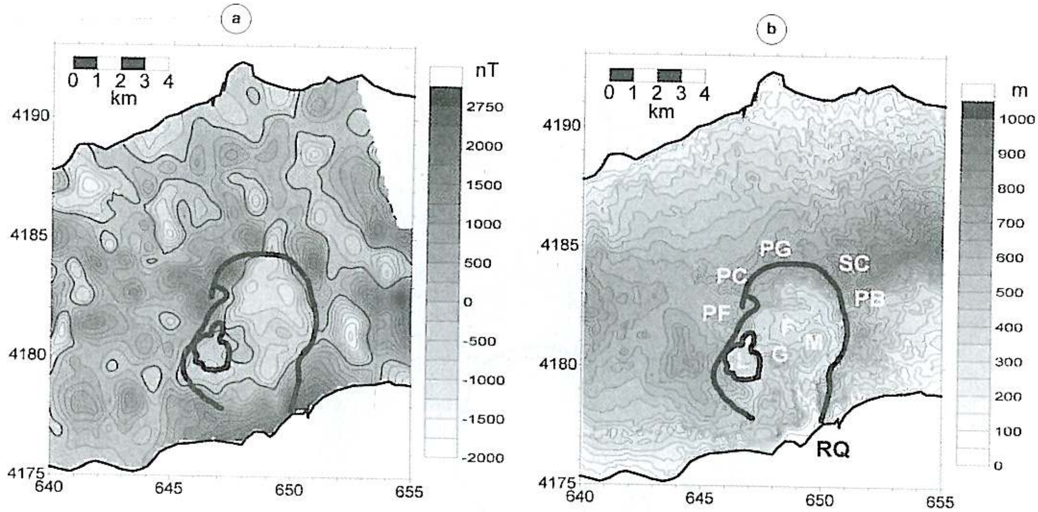

Fig. 6a,b. a) Reduced to the pole magnetic anomaly map of Furnas caldera and surrounding areas obtained from the land magnetic data; b) topographic map of the same area, where L = Lagoa das Furnas (Furnas lake); F = Furnas village; G = Pico do Gaspar; M = Pico das Marconas; RQ = Ribeira Quente village; PF = Pico do Ferro; PC = Pico Ceguinho; PG = Pico Grande; PB = Pico do Buraco; SC = Salto do Cavalo.

5.3. *Magnetic layers*

Spectral analysis is a widely-used technique for the estimation of the depth to the magnetic sources, as the formula of magnetic anomalies is considerably simpler in the wavenumber domain. The most typical processing techniques consider statistical models, and are generally based on the method developed by Spector and Grant (1970). However, for its simplicity, we have applied the method of Okubo and Shibuya (1993). Assuming that the magnetic source is a bidimensional body, these authors deduced a very simple linear expression which relates the power spectrum of the magnetic anomaly with the depth to the source. Beginning with the formula of the power spectrum of a rectangular prismatic body (Bhattacharyya and Leu, 1975), they obtained the following expression introducing some hypotheses:

$$\ln\left[\frac{P(k)^{1/2}}{k}\right] = A - k z_0. \qquad (5.1)$$

This is valid when $ka \ll 1$, $kD \ll 1$ and $\cot\psi \leq 1$, where: $P(k)$ is the power spectrum of the magnetic anomaly; k is the wavenumber; A is a constant; a is the horizontal half-thickness of the body; D is the vertical half-thickness of the body; ψ is the inclination angle of the body; and z_0 is the centroid depth of the body. This expression shows that it is possible to obtain the centroid depth of the source directly from the gradient of the spectrum.

In the same way, the following relation can be written (Okubo *et al.*, 1985):

$$\ln\,[P(k)^{1/2}] = B - k z_t. \qquad (5.2)$$

Where B is a constant and z_t is the depth to the top of the body. Again, we see that it is straightforward to obtain the depth to the top of the source by means of the anomaly power spectrum. It is simple to calculate the depth to the bottom of the source, z_b with the expression $z_b = 2z_0 - z_t$.

Three profiles, which cross the most significant anomalies, were selected to apply this method, and are shown in fig. 5. The power

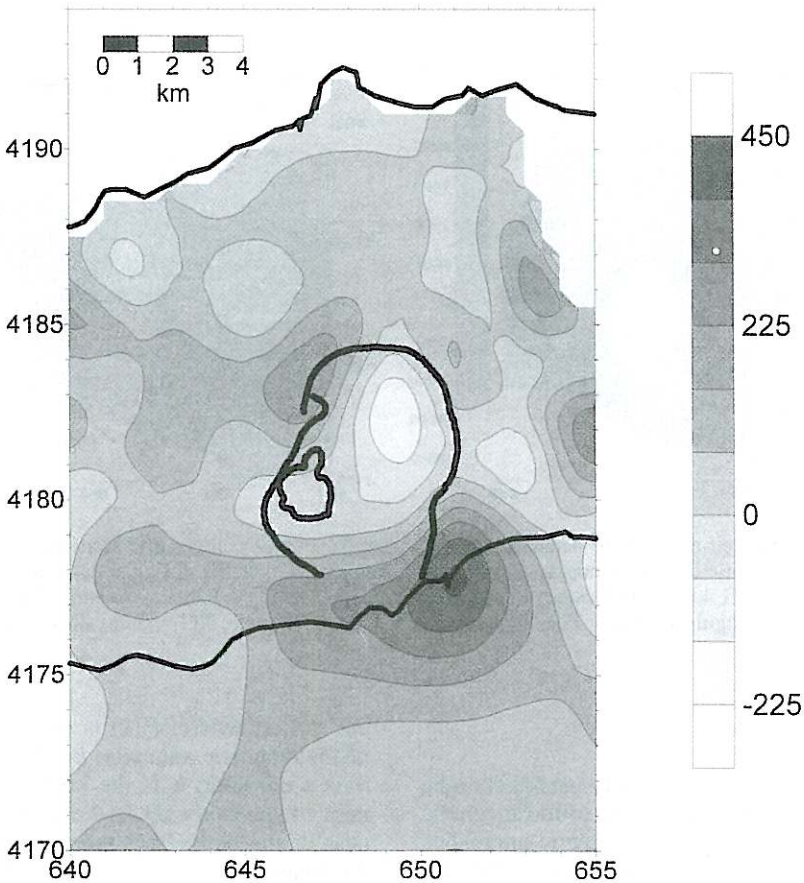

Fig. 7. Upward continuation to 2 km a.s.l. of the pseudogravity map of Furnas caldera and surrounding areas obtained from land and marine data.

spectra were calculated with a FFT algorithm, and both ln $[P(k)^{1/2}/k]$ and ln $[P(k)^{1/2}]$ *versus* k were plotted. Finally, a linear fit was performed to obtain z_0 and z_t (fig. 8). When interpreting these results, however, we must keep in mind that the initial hypothesis of a 2D structure may be quite restrictive.

5.4. *Forward modelling*

A 2.5D forward method was applied to fit the synthetic anomaly caused by a certain structure to the anomaly observed along the profile A-A′. For this purpose, the GRAVMAG (1993) program was used. This program provides the magnetic anomaly along a profile assuming that the anomalous bodies are finite prisms of polygonal cross-section and uniform magnetization. The expressions for these anomalies were taken from Shuey and Pasquale (1973). First, the anomaly created by a uniformly-magnetized topography was obtained (fig. 9), with the aim of quantifying the effect of the terrain. Second, after taking into account all the previous information obtained about the sources, a structural magnetic model was constructed along the same profile (fig. 10).

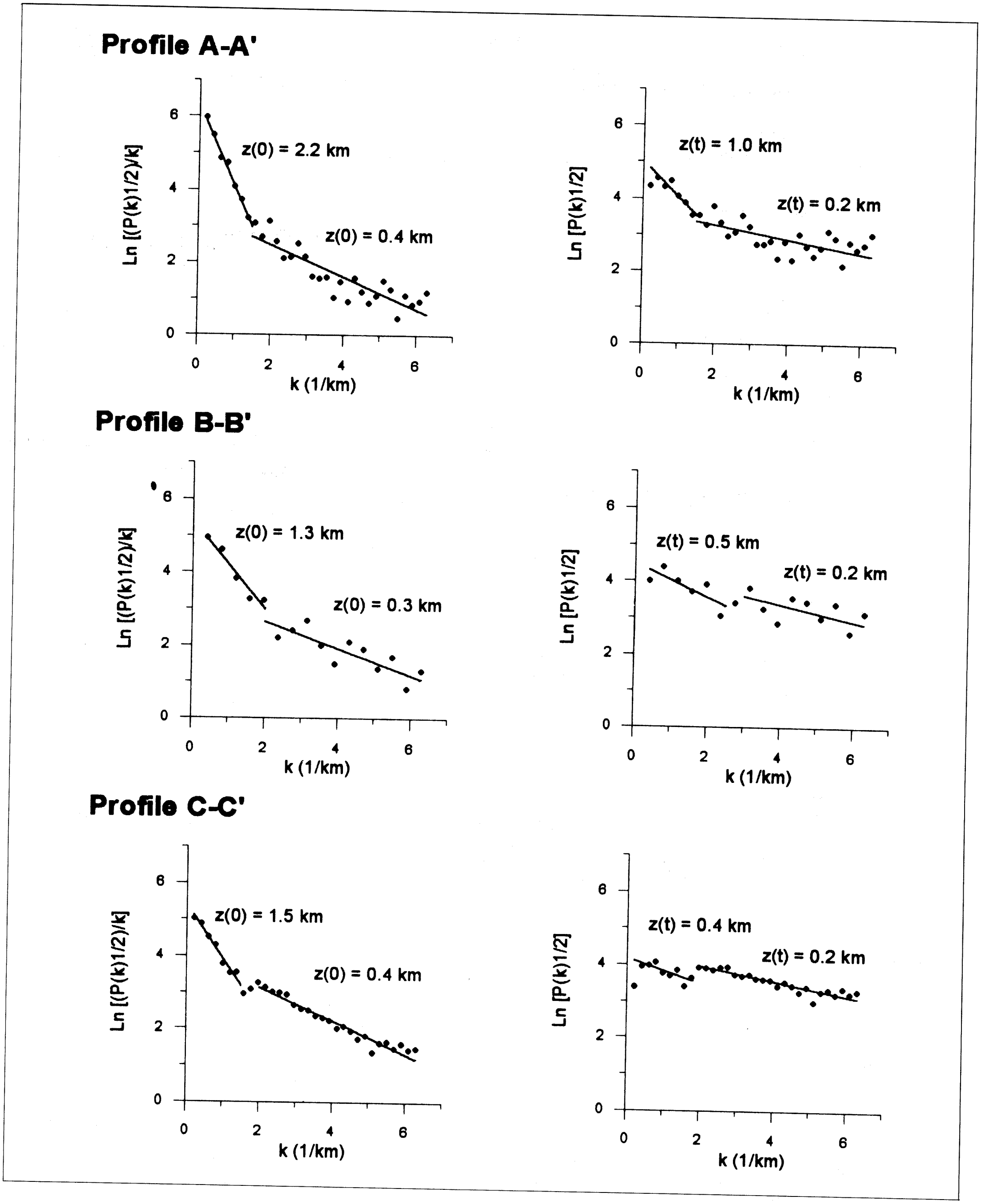

Fig. 8. Magnetic anomaly power spectra along the profiles shown in fig. 5 and depths obtained for the anomalous bodies: $z(t)$ = depth to the top; $z(0)$ = depth to the centre (or centroid depth).

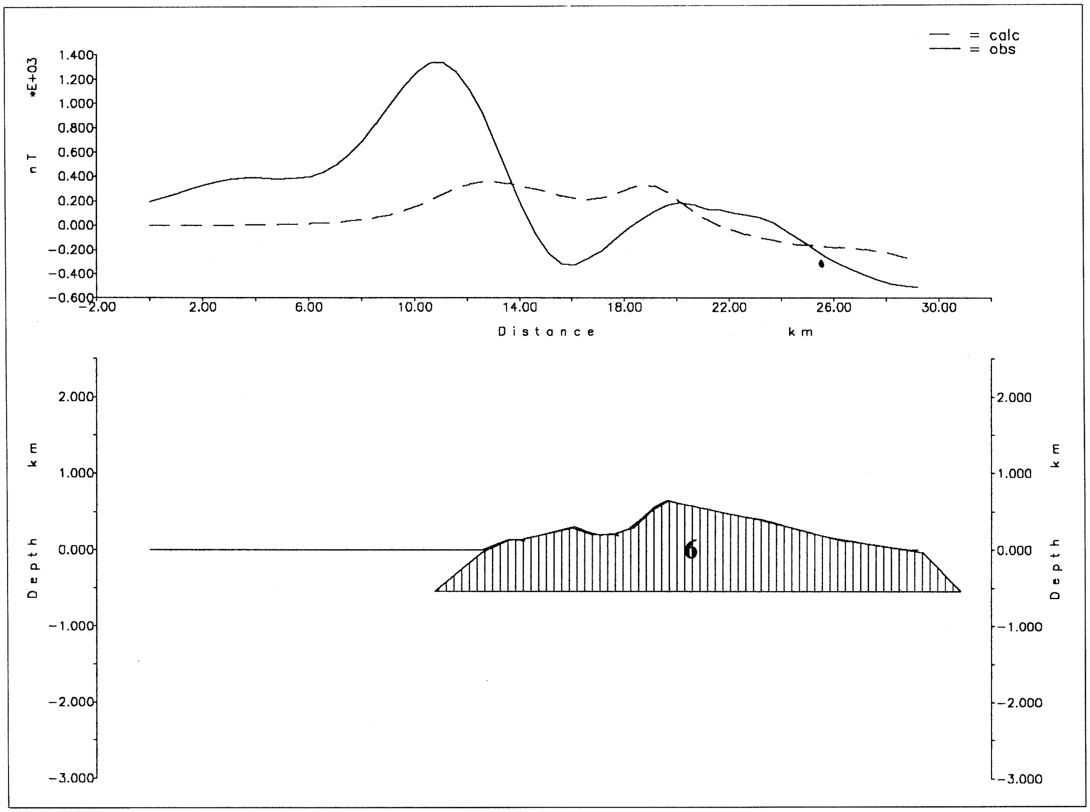

Fig. 9. Comparison between the upwardly-continued magnetic anomaly map (black line) and the synthetic anomaly (dashed line) created by a topography characterized by a constant total magnetization of 6 Am^{-1} along the profile A-A′ (see fig. 5).

6. Discussion

The magnetic anomaly map shown in fig. 4 is complex, as results from the superposition of many high-amplitude anomalies (several thousand nT) characterized by different wavelengths. This is expected as magnetic sources have different sizes, different magnetization contrasts and are located at different depths.

The interpretative techniques described above have provided some information about the sources, especially concerning their size and location. Nevertheless, this must be used carefully, as it has been necessary to assume some hypotheses in the processing of the map which, in some cases, could be not completely verified.

6.1. *Shallow structures*

If we compare the magnetic anomaly map and the topographic map it is possible to appreciate a certain correlation between them. This becomes clearer when the map is reduced to the pole (fig. 6a,b). In general, the higher elevation areas seem to be related to positive values of residual magnetic field, while over the inner part of the caldera, for example, they

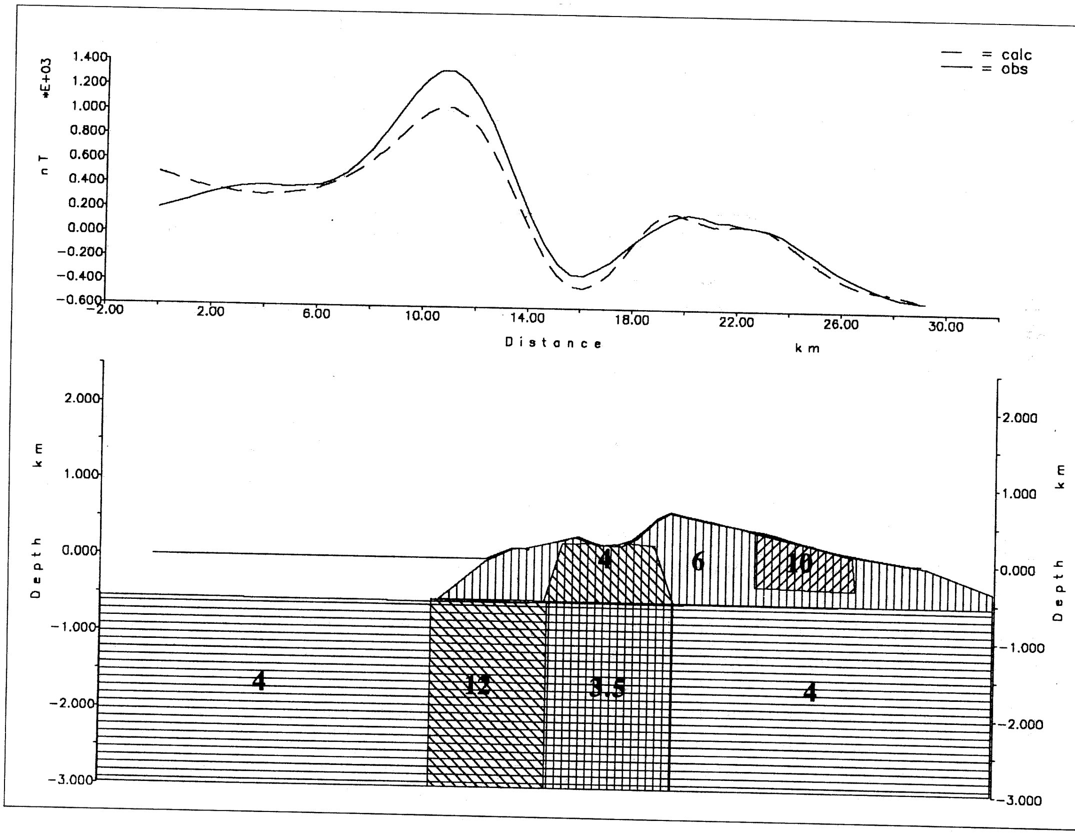

Fig. 10. Comparison between the upwardly-continued magnetic anomaly map (black line) and the synthetic anomaly (dashed line) created by the structure that appears in the figure, where the numbers correspond to total magnetizations in Am^{-1} along the A-A′ profile (see fig. 5).

are negative. This important shallow contribution is expected in any volcanic area, especially when it is a quaternary structure, as is the case of Furnas. However, the topography is not the only magnetic source. Figure 9 shows the magnetic anomaly observed along A-A′ profile and the synthetic one due to a uniformly magnetized topographic layer. This is only a first approximation, but it allows us to state that, although there is some similarity, they are quite different. Moore (1983, 1991) points out in the geological map of Furnas that the caldera and surrounding areas are widely covered by trachytic pyroclasts. The values of susceptibility and NRM measured for this kind of materials (table I, samples 1 and 3) reveal very low magnetizations, as expected for such light products. The correlation between magnetic anomalies and topography prove that these materials constitute a very thin layer overlying denser materials (lava flows, domes, ignimbrites), which are responsible for the high magnetization of shallow origin.

In the inner part of the caldera, two different zones of negative anomaly are distinguished: one is detected over Furnas Lake, while the lowest values of the caldera appear in the immediate neighbourhood of Furnas village (fig. 4 and 6a). Pseudogravity integration separates both zones, pointing out that the main source should be near Furnas village (fig. 7). The domes named Pico do Gaspar and Pico das Marconas are revealed in the reduced to the pole magnetic anomaly map as small highs in comparison with the surrounding values of residual magnetic field. In the north of the caldera, the negative anomaly continues outside the caldera wall. This indicates a different source from the unevenness of the relief.

The outer part of the caldera shows a series of small highs which corresponds to a dome alignment near the northwest (Pico do Ferro, Pico do Ceguinho, Pico Grande) and northeast caldera rim (Pico do Buraco) (fig. 4 and 6a). The intensities of these small highs seem to be related to their composition: the highest ones are associated to mafic domes (Pico do Ceguinho, Pico Grande, Pico do Buraco), while their intensity is lower for the trachytic ones (Pico do Gaspar, Pico das Marconas). Sample No. 8, which belongs to the hawaiitic deposits of Salto do Cavalo-Pico do Buraco, is characterized by a strong susceptibility. There is one exception: the Pico do Ferro dome which, in spite of being formed by trachytic materials, is associated to a more intense anomaly. This difference could be due to the different material the domes overlie, as the size and age of the cones are similar. In fact, Moore (1991) suggests that Pico do Ferro could be emplaced over a tristanite flow. In this case, the general law that associates greater anomalies to salic materials rather than to mafic ones when oxidation processes have not taken place (Haggerty, 1979) is not verified. This fact suggests that some oxidation must have occurred.

6.2. *Deep structures*

Upward continuation filtered short-wavelength anomalies favouring the effect of relatively deep sources (fig. 5). The most remarkable features are the negative values that appear within the caldera (now it is not possible to distinguish between the two zones mentioned before) and the intense high that appears to the south of the coast. The appearance of these anomalies leads to the conclusion that both are caused by the same structure (*i.e.*, a strongly-magnetized body beneath the south coast). In fact, the azimuth of the imaginary line which connects both anomalies is almost coincident with the magnetic declination in São Miguel ($-11°$), and it seems reasonable that the magnetization of this anomalous body is approximately parallel to the present field. If this is true, pseudogravity integration would transform the magnetic anomaly into a pseudogravity high located over the source somewhere between the magnetic high and the low. However, the transformed map displays both a pseudogravity maximum and a minimum, pointing out that two different sources are present. This means that it is likely that a strongly-magnetized body exists below the south coast (the reason for the maximum), as well as a structure characterized by a negative magnetization contrast beneath the caldera (which produces the minimum). Nevertheless, it is necessary to take into account that the distribution of marine data does not allow the intensity or size of the magnetic high to be precisely defined.

The spectral analysis based on the method of Okubo and Shibuya (1993) can be applied to linear anomalies, as it assumes a two-dimensional source. In a first approximation, three profiles which cross the caldera were selected (fig. 5). The linear fits of spectra and estimated depths are shown in fig. 8. In all the profiles it is easy to distinguish two different magnetized layers (which are worse defined in the C-C′ profile). The magnetic horizon separating them is at an average depth of 0.8 km. Thus, we can imagine a shallow layer which extends from the surface to this depth, and a deeper one from there on. These results are coherent with the structure proposed by Forjaz (1986), who suggests that the interface between Furnas materials and the submarine lavas overlaid by them is located at a depth of approximately 1 km. This result was integrated in the structural forward model, as well as all the characteristics of the magnetic sources deduced from the different interpretative techniques.

Taking into account that the transformations applied to the anomaly map especially emphasize the above mentioned anomaly, the structural model was constructed along the A-A′

profile. The main problem of this task in a place such as Furnas is the lack of geological and geophysical data to support the hypotheses. The existence of a body at high temperature somewhere beneath the caldera is evident, as it must be the source of heat for the fumaroles and thermal springs at the surface. In the same way, a reservoir where the original basaltic magma has evolved to the acidic one, responsible for the typical trachytic eruptions of Furnas, must exist. Machado (1973) states that this magma chamber must be emplaced at a depth of about 5 km, but it is not clear how he reaches this conclusion. If this assertion is true, the shallow character of this study does not allow a body to be detected at such depth. Sigmundson *et al.* (1995) detected, from GPS and optical levelling tilt data, a small inflation greater than 7 mm/yr inside the caldera, and suggest that it may be caused by accumulation of magma at shallow depth beneath the caldera. However, they do not reject the possibility that it could be due to fluid accumulation within a deep hydrothermal system beneath the caldera. On the other hand, there are no well logs which reveal the dependence of the magnetic properties of rocks on depth, or seismic studies that provide information about the structure of the crust in this area. The number of rock samples that were collected may not be representative of the magnetic properties of the entire volume of the volcano. Keeping all this in mind, the proposed model is only one of the possible structures along a profile which could be representative (fig. 10). This is a simple model, as more detail will not necessarily mean more resolution and accuracy, as it would not be supported by real data.

It is necessary to note that the applied forward modeling technique assumes that the structures are symmetric with respect to the profile direction. Therefore, although the anomalies show a quasi-axial behaviour with respect to this direction, we must not forget that real sources may not be so symmetric as we presumed. The initial fixed parameters of the modelling were: 1) the location of the horizontal contrast between the materials of Furnas and the oceanic lavas at a depth of 500 m b.s.l.; 2) the average magnetization of the terrain: as trachyte is the most abundant rock (Moore, 1991), measurements obtained in the laboratory for this kind of material have been considered typical. Taking into account that, even the upwardly-continued map contains information from the topography, the shallowest materials were characterized by a high total magnetization (remanent + induced) of 6 Am^{-1}; 3) the magnetization of the basaltic oceanic lavas: a typical value of 4 Am^{-1} for this kind of material was assumed (Reynolds *et al.*, 1990). Starting with this initial simple model, several structures, based on reliable assumptions, were added in order to fit the synthetic anomaly to the actual data (fig. 10).

To explain the secondary high that appears to the north of the caldera, a total magnetization of 10 Am^{-1} has been assumed. This could be related to the presence of basaltic materials in the northern part of the volcano (Moore, 1983). On the other hand, the evident existence of an active hydrothermal system which must affect the caldera filling materials, led us to assume that the alterations that the hydrothermal fluids produce on the magnetic minerals are, at least in part, the origin of the wide magnetic low.

Several authors have associated magnetic lows with the decrease of magnetization due to alteration of hydrothermal origin (Smith *et al.*, 1974; Kane *et al.*, 1976; Criss and Champion, 1984; Rapolla *et al.*, 1989; Hildebrand *et al.*, 1993). This effect mainly consists of the oxidation of the ferromagnetic minerals which are transformed into paramagnetic or antiferromagnetic ones when fluids at high temperature (200-300°C) circulate within the rocks. A typical transformation would be the oxidation of magnetite to produce hematite. However, the exact mechanism of this process is not very well understood, as sometimes the result is an enhancement of magnetic moment. For example, Criss and Champion (1984), studying the Idaho batholith, observed the crystallization of secondary magnetite as a consequence of the precipitation of iron from the hydrothermal fluids. This effect was also described by Hall and Fisher (1988). The exact conditions which produce one process or the other are not very well known, so it is not possible to assure that hydrothermal alteration always decreases the magnetization of the rocks. This type of alteration undoubtedly exits in Furnas (Malheiro *et al.*, 1993), but there is no information about its effect on magnetic minerals. The samples we collected in the field and studied in the laboratory belong to fresh rocks so, unfortunately, do not aid in ascertaining the influence of hydrothermalism on the magnetic petrology in Furnas caldera.

Magnetic lows can have other causes. Reversely-magnetized rocks or temperatures above the Curie point are often the source of negative anomalies: the former because they create a magnetic field opposite to the present main field, and the latter because these rocks have no magnetization. In both cases, the magnetization contrast with respect to the surrounding rocks would be negative. Both circumstances have been rejected in Furnas. The age of the volcano restricts the acquisition of remanence to a period where the polarity of the main field has remained normal (Furnas has been almost entirely constructed over the past 100000 years (Moore, 1991), while the last reversal occurred 750000 years ago (*e.g.*, Parkinson, 1983)). On the other hand, the oceanic lavas below Furnas are magnetized in the normal direction, as revealed by the map of marine anomalies of this area. Taking this into account, it is clear that a reversed magnetization cannot be the cause of the magnetic low over Furnas caldera.

The size of the area covered by the magnetic survey restricts the depth to the magnetic sources to approximately the first 3 km. Thus, if rocks at temperatures higher than the Curie point exist within this 3 km-layer they will contribute to the broad magnetic low over the caldera. The first question is: what temperature is the Curie point for these rocks? The values obtained for the rock samples are very variable and, in some cases, range from 225° to 280°C (corresponding to titanomagnetite with low degree of oxidation). These temperatures are in the interval of temperatures of the hydrothermal fluids. In the neighbouring volcano Fogo-Agua de Pau, temperatures of 240°C for these fluids have been measured at a depth of 500-1000 m (Gandino *et al.*, 1985). Unfortunately, there are no data about the vertical distribution of temperature in Furnas. But considering the closeness (a few kilometers) and similarities between both volcanoes, it is possible to assume that the vertical temperature profiles should be of the same kind. However, the effect of hydrothermal oxidation on the Curie temperatures is always a rise, as titanomagnetite looses titanium and approximates to pure magnetite (Ade-Hall *et al.*, 1971; O'Reilly, 1984). That is, altered rocks are characterized by higher Curie temperatures than fresh rocks. Consequently, it is unlikely that rocks at temperatures of a few hundreds degrees Celsius have lost their magnetic properties as a result of overtaking the Curie point.

Bearing in mind all these reasonings, we have considered that, at least a portion of the magnetic low observed over Furnas caldera (especially in the northern part) is originated by the oxidation of magnetite as a result of hydrothermal oxidation. Therefore, the materials filling the caldera have been assigned a magnetization lower than that of the surrounding ones. As the fluid circulation seems to be more active in the first kilometer (Lawrence and Maxwell, 1978, measured the greatest concentration of fluids at 600-700 m in Fogo close volcano), a slightly lower magnetization contrast has been considered for the deeper materials. For this assumption we also took into account that at depths greater than about 1 km the nature of rocks is different (basalts instead of trachytes), and that the temperatures and concentration of hot fluids should be different too.

To explain the origin of the large magnetic high to the south of the island it is necessary to include a strongly-magnetic body in the model (M = 12 Am^{-1}), emplaced below the south coast as inferred from the pseudogravity map (fig. 7). This magnetic body is, of course, source for some of the negative anomaly inside the caldera. The origin of this body is not straightforward. It could be, for example, a trachytic intrusion emplaced amongst the basaltic lavas which did not reach the surface. Once this magma was emplaced, the slow cooling would favour deuteric oxidation and ex-solution, transforming initial titanomagnetite into almost pure magnetite and, consequently, increasing its magnetic moment. This could be an explanation for the acquisition of a high remanent magnetization.

7. Conclusions

The local magnetic anomaly study of Furnas caldera has disclosed the existence of important magnetic anomalies in this area which are related to the different structures of the volcano. This result will be useful to improve our understanding of this hazardous volcano. The most important conclusions that can be derived from this work are summarized as follows:

– A rather good correlation between the magnetic anomaly map and the topographic map is observed. This implies that the shallowest materials are characterized by strong magnetizations, as could be expected for such a young volcano.

– The short-wavelength positive anomalies are related to mafic domes (Pico do Ceguinho, Pico Grande, Pico do Buraco), while they are not so intense when the domes are of trachytic composition (Pico do Gaspar, Pico das Marconas). There is one exception: Pico do Ferro. Although it is a trachytic dome, it appears associated with a high positive anomaly. This fact could be connected to the existence of a tristanite flow overlaid by the dome.

– It was not possible to detect, at least at first, the main fault system of the area (WNW-ESE). This is probably because these fractures exclusively affect the shallowest pyroclastic deposits.

– The inner part of the caldera is characterized by a broad negative magnetic anomaly. The origin of this low magnetization could be related to the oxidation of the magnetic minerals as a result of hydrothermal alteration processes. This alteration would affect the shallowest materials more intensively (from the surface to perhaps 500 m b.s.l. (Forjaz, 1996)), where the hydrothermal system seems more active, but its effect probably exists at a depth of some kilometers. The minimum magnetic field value within the caldera is reached in the neighbourhood of Furnas village, and could be related to the fumaroles and, consequently, to the fractures where the hydrothermal fluids circulate. It is noteworthy that Sigmundsson *et al.* (1995) suggest that the center of the deformation they detected by means of geodetic techniques is located in this zone.

– Although it is not possible to define it precisely because of the lack of data in this area, a strongly magnetized body located beneath the south coast of the island was detected. This body could be a trachytic intrusion emplaced within the oceanic basaltic materials.

– A magnetization contrast at a depth of approximately 1 km was detected, which corresponds to the interface between Furnas materials and the oceanic lavas which lie beneath them (Forjaz, 1986).

– The magma chamber, presumed to be at about 5 km beneath the caldera, was not detected from the magnetic anomaly map, as this provides information only from approximately the first 3 km.

– The most intense negative anomalies of the entire area were measured in the Povoaçao neighbouring caldera, which is considered to be extinct at present. This high minimum could be due to rocks magnetized during a period of reversed polarity of the main field.

Acknowledgements

The authors are indebted to A. Galdeano for providing his routines to transform the anomaly maps. S. Macmillan and D.R. Barraclough are also acknowledged for their adapted version of the same routines. Also, we wish to thank M.L. Osete for kindly allowing us to use the equipment of the Paleomagnetism Laboratory of the Universidad Complutense of Madrid for the magnetic analysis of the rock samples.

REFERENCES

ADE-HALL, J.M., H.C. PALMER and T.P. HUBBARD (1971): The magnetic and opaque petrological response of basalts to regional hydrothermal alteration, *Geophys. J. R. Astron. Soc.*, **24**, 137-174.

ARKANI-HAMED, J. (1988): Differential reduction-to-the-pole of regional magnetic anomalies, *Geophysics*, **53**, 1592-1560.

BARANOV, V. (1957): A new method for interpretation of aeromagnetic maps: pseudo gravimetric anomalies, *Geophysics*, **22**, 359-383.

BARBERI, F., A. GANDINO, A. GIONCADA, P. LA TORRE, A. SBRANA and C. ZENUCCHINI (1994): The deep structure of the Eolian arc (Filicudi-Panarea-Vulcano sector) in light of gravity, magnetic and volcanological data, *J. Volcanol. Geotherm. Res.*, **61**, 189-206.

BHATTACHARYYA, B.K. and K.C. CHAN (1977): Reduction of magnetic and gravity data on an arbitrary surface acquired in a region of high topographic relief, *Geophysics*, **42**, 1411-1430.

BHATTACHARYYA, B.K. and L.K. LEU (1975): Analysis of magnetic anomalies over Yellowstone National Park: mapping of Curie point isothermal surface for geothermal reconnaissance, *J. Geophys. Res.*, **80**, 4461-4465.

BLAKELY, R.J. (1981): A program for rapidly computing the magnetic anomaly over digital topography, *U.S. Geological Survey Open-File Report*, **81-298**.

BOOTH, B., G.P.L. WALKER and R. CROASDALE (1978): A quantitative study of five thousand years of volcanism on S. Miguel, Azores, *Philos. Trans. R. Soc. London, Ser. A*, **V228**, 271-319.

CAMPOS-ENRIQUEZ, J.O. and V.H. GARDUÑO-MONROY (1995): Los Azufres silicic center (Mexico): inference of caldera structural elements from gravity, aeromagnetic and geoelectrical data, *J. Volcanol. Geotherm. Res.*, **67**, 123-152.

CLARKE, G.K.C. (1971): Linear filters to suppress terrain effects on geophysical maps, *Geophysics*, **36**, 963-966.

COELHO, E.P. (1968): Trabalhos gravimétricos no arquipélago dos Açores, *Cad. Técn. Inf.*, No. 14, Inst. Geogr. Cadastral, Lisboa.

CRISS, R.E. and D.E. CHAMPION (1984): Magnetic properties of granitic rocks from the southern half of the Idaho batholith: influences of hydrothermal alteration and implications for aeromagnetic interpretation, *J. Geophys. Res.*, **89**, 7061-7076.

FORJAZ, V.H. (1984): *S. Miguel: Volcanostratigraphic Sketch*, Univ. dos Açores, P. Delgada.

FORJAZ, V.H. (1986): *Corte Geológico Esquemático da Ilha de S. Miguel*, Univ. dos Açores, P. Delgada.

FORJAZ, V.H. (1996): Geothermal reservoirs of Furnas Laboratory Volcano, presented at the *2nd Workshop on European Laboratory Volcanoes, Santorini, Greece, 2-4 May 1996*.

GANDINO, A., M. GUIDI, C. MERLO, L. METE, R. ROSSI and L. ZAN (1985): Preliminary model of the Ribeira Grande geothermal field (Azores Islands), *Geothermics*, **14**, 91-105.

GASPAR, J.L., T. FERREIRA, G. QUEIROZ, J. GUEST, N. WALLENSTEIN, J. PACHECO, A. DUNCAN and P. COLE (1996): Main tectonic structures of Furnas volcano (So Miguel, Azores), presented at the *2nd Workshop on European Laboratory Volcanoes, Santorini, Greece, 2-4 May 1996*.

GIBERT, D. and A. GALDEANO (1985): A computer program to perform transformations of gravimetric and aeromagnetic surveys, *Comput. Geosci.*, **11**, 553-588.

GRAUCH, V.J.S. (1987): A new variable-magnetization terrain correction method for aeromagnetic data, *Geophysics*, **52**, 94-107.

GRAVMAG v1.5 (1993): British Geological Survey, Nottingham, U.K.

GUEST, J.E., A.M. DUNCAN, P.D. COLE, J.L. GASPAR, G. QUEIROZ, N. WALLESTEIN and T. FERREIRA (1994): Preliminary report on the volcanic geology of Furnas volcano, S. Miguel, The Azores, in *Furnas European Laboratory Volcano Progress Report*, edited by V.H. FORJAZ, Univ. dos Açores.

HAGGERTY, S.E. (1979): The aeromagnetic mineralogy of igneous rocks, *Can. J. Earth Sci.*, **16**, 1281-1293.

HALL, J.M. and B.E. FISHER (1988): The iceland drilling project crustal section, stable remagnetization below 3 km crustal depth, *Can. J. Earth Sci.*, **25**, 1304-1315.

HILDEBRAND, T.G., J.G. ROSENBAUM and J.P. KAUAHIKAUA (1993): Aeromagnetic study of the island of Hawaii, *J. Geophys. Res.*, **98**, 4099-4119.

HOOVER, D., R. AMARAL and M. BROKER (1983): Preliminary report on audio-magnetotelluric survey on São Miguel Island, Azores, Portugal, *US Geological Survey Open-File Report*, **83-441**.

IAGA DIV. V, WORKING GROUP 8 (1992): International geomagnetic reference field, 1991 revision, *Geophysics*, **57**, 956-959.

JACOBSEN, B.H. (1987): A case for upward continuation as a standard separation filter for potential-field maps, *Geophysics*, **52**, 1138-1148.

KANE, M.F., D.R. MABEY and R.L. BRACE (1976): A gravity and magnetic investigation of the Long Valley Caldera, Mono County, California, *J. Geophys. Res.*, **81**, 754-762.

KRAUSE, D. and N. WATKINS (1970): North Atlantic crustal genesis in the vicinity of the Azores, *Geophys. J. R. Astron. Soc.*, **9**, 261-283.

LAWRENCE, J.R. and S. MAXWELL (1978): Geothermal exploration in the Azores: $^{18}O/^{16}O$ in calcites from volcanic rocks, *J. Volcanol. Geotherm. Res.*, **4**, 219-223.

LENAT, J.F. and M. AUBERT (1982): Structure of Piton de la Fournaise volcano (La Reunion Island, Indian Ocean) from magnetic investigations. An illustration of the analysis of magnetic data in a volcanic area, *J. Volcanol. Geotherm. Res.*, **12**, 361-392.

MACHADO, F. (1959): Submarine pits of the Azores Plateau, *Bull. Volcanol.*, **21**, 109-116.

MACHADO, F. (1973): Acid volcanoes of San Miguel, Azores, *Bull. Volcanol.*, **36**, 319-327.

MALHEIRO, A.M., J.M. VIEIRA E SILVA and A.M. GALOPIM DE CARVALHO (1993): Caracterização químico-mineralógica de amostras do complexo vulcânico das Furnas (Açores), *Gaia*, **7**, 1-5.

MOORE, R.B. (1983): Preliminary geological map of Furnas volcano, São Miguel, Azores, *US Geological Survey Open-File Report*, **83-395**, scale 1:15000.

MOORE, R.B. (1991): Geology of the three late Quaternary stratovolcanoes on S. Miguel, Azores, *US Geological Survey Bulletin*, **1900**.

MUROI, I. (1973): Results of aeromagnetic surveys over volcanoes and calderas in Japan, *Sci. Rep. Tohoku Univ. Ser. 5 Geophysics*, **21**, 87-111.

NISHIDA, Y. (1984): Subsurface structure of Toya Caldera, Japan, as revealed by detailed magnetic survey, *J. Phys. Earth*, **32**, 423-434.

NISHIDA, Y. and E. MIYAJIMA (1984): Subsurface structure of Usu volcano, Japan, as revealed by detailed magnetic survey, *J. Volcanol. Geotherm. Res.*, **22**, 271-285.

NUNZIATA, C. and A. RAPOLLA (1987): A gravity and magnetic study of the volcanic island of Ischia, Naples (Italy), *J. Volcanol. Geotherm. Res.*, **31**, 333-344.

OKUBO, Y. (1994): Magnetic modeling of the Hakkoda volcanoes, Japan, *J. Geomagn. Geoelectr.*, **46**, 513-528.

OKUBO, Y. and A. SHIBUYA (1993): Thermal and crustal structure of the Aso volcano and surrounding regions constrained by gravity and magnetic data, Japan, *J. Volcanol. Geotherm. Res.*, **55**, 337-350.

OKUBO, Y., R. GRAF, R.O. HANSEN, K. OGAWA and H. TSU (1985): Curie point depths of the island of Kyushu and surrounding areas, Japan, *Geophysics*, **50**, 481-494.

O'REILLY, W. (1984): *Rock and Mineral Magnetism* (Blackie, Glasgow), pp. 220.

ORTIZ, R., J. VILA, A. GARCIA, A.G. CAMACHO, J.L. DIEZ, A. APARICIO, R. SOTO, J.G. VIRAMONTE, C. RISSO, N. MENEGATTI and I. PETRINOVIC (1992): Geophysical features of Deception Island, in *Recent Progress in Antartic Earth Science*, edited by Y. YOSHIDA, K. KAMINUMA and K. SHIRAISHI (TerraPub, Tokyo), 443-448.

PARKINSON, W.D. (1983), *Introduction to Geomagnetism* (Scottish Academic Press, Edinburgh), pp. 433.

PLOUFF, D. (1976): Gravity and magnetic fields of polygonal prisms and application to magnetic terrain corrections, *Geophysics*, **41**, 727-741.

QUINTINO, J.D. (1962): Levantamento geomagnético da ilha de S. Miguel (Açores), RT 638, GEO 19, Serv. Meteor. Nac., Lisboa.

RAPOLLA, A., M. FEDI and M.G. FIUME (1989): Crustal structure of the Ischia-Phlegrean geothermal fields, near Naples, Italy, from gravity and aeromagnetic data, *Geophys. J.*, **97**, 409-419.

REYNOLDS, R.L., J.G. ROSENBAUM, M.R. HUDSON and N.S. FISHMAN (1990): Rock magnetism, the distribution of magnetic minerals in the Earth's crust and aeromagnetic anomalies, in *Geologic Applications of Modern Aeromagnetic Surveys, U.S. Geologic Survey Bulletin*, 1924, pp. 25-45.

SHUEY, R.T. and A.S. PASQUALE (1973): End corrections in magnetic profile interpretation, *Geophysics*, **38**, 507-512.

SIGMUNDSSON, F., E. TRYGGVASON, M.M. ALVES, J.L. ALVES, K. PALSSON and H. OLAFSSON (1995): Slow inflation of the Furnas volcano, São Miguel, Azores, suggested from initial leveling and Global Positioning System measurements, *Geophys. Res. Lett.*, **22**, 1681-1684.

SMITH, R.B., R.T. SHUEY, R.O. FREIDLINE, R.M. GTIS and L.G. ALLEY (1974): Yellowstone hot spot: new magnetic and seismic evidence, *Geology*, **2**, 451-455.

SPECTOR, A. and F.S. GRANT (1970): Statistical models for interpreting aeromagnetic data, *Geophysics*, **35**, 293-302.

WATKINS, N.D. and T.P. PASTER (1971): The magnetic properties of igneous rocks from the ocean floor, *Philos. Trans. R. Soc. London, Ser. A*, **268**, 507-550.